



Published in final edited form as:

Placenta. 2008 September ; 29(9): 790–797. doi:10.1016/j.placenta.2008.06.005.

Modeling the variability of shapes of a human placenta:

December 28, 2007

Michael Yampolsky¹, Carolyn M. Salafia^{2,3}, Oleksandr Shlakter⁴, Danielle Haas⁵, Barbara Eucker⁶, and John Thorp⁶

¹Department of Mathematics, University of Toronto, 40 St. George St, Toronto, Ontario, Canada, M5S2E4

²Department of Psychiatry, New York University School of Medicine. 550 First Avenue, New York, NY 10016

³Department of Obstetrics and Gynecology, St Luke's Roosevelt Hospital, NY, NY, 10019.

⁴Department of Mechanical and Industrial Engineering, University of Toronto, 5 King's College Road, Toronto, Ontario, Canada M5S3G8

⁵Department of Pathology, St Luke's Roosevelt Hospital, NY, NY, 10019

⁶Department of Obstetrics and Gynecology, University of North Carolina at Chapel Hill, Chapel Hill, NC 27599

Abstract

Background—Placentas are generally round-oval in shape, but “irregular” shapes are common. In the Collaborative Perinatal Project data, irregular shapes were associated with lower birth weight for placental weight, suggesting variably shaped placentas have altered function.

Methods—(I) Using a 3-D one-parameter model of placental vascular growth based on Diffusion Limited Aggregation (an accepted model for generating highly branched fractals), models were run with a branching density growth parameter either fixed or perturbed at either 5-7% or 50% of model growth. (II) In a data set with detailed measures of 1207 placental perimeters, radial standard deviations of placental shapes were calculated from the umbilical cord insertion, and from the centroid of the shape (a biologically arbitrary point). These two were compared to the difference between the observed scaling exponent and the Kleiber scaling exponent (0.75), considered optimal for vascular fractal transport systems. Spearman's rank correlation considered $p < 0.05$ significant.

Results—(I) Unperturbed, random values of the growth parameter created round-oval fractal shapes. Perturbation at 5-7% of model growth created multilobate shapes, while perturbation at 50% of model growth created “star-shaped” fractals. (II) The radial standard deviation of the perimeter from the umbilical cord (but not from the centroid) was associated with differences from the Kleiber exponent ($p = 0.006$).

Conclusions—A dynamical DLA model recapitulates multilobate and “star” placental shapes via changing fractal branching density. We suggest that (1) irregular placental outlines reflect deformation of the underlying placental fractal vascular network, (2) such irregularities in placental outline indicate sub-optimal branching structure of the vascular tree, and (3) this accounts for the lower birth weight observed in non-round/oval placentas in the Collaborative Perinatal Project.

Corresponding author: Michael Yampolsky, PhD Department of Mathematics University of Toronto 40 St. George Street, Toronto, Canada M5S2E4 Email: Michael.yampolsky@gmail.com.

Publisher's Disclaimer: This is a PDF file of an unedited manuscript that has been accepted for publication. As a service to our customers we are providing this early version of the manuscript. The manuscript will undergo copyediting, typesetting, and review of the resulting proof before it is published in its final citable form. Please note that during the production process errors may be discovered which could affect the content, and all legal disclaimers that apply to the journal pertain.

INTRODUCTION

The placenta is the primary fetal source of oxygen and nutrients. As such, it is a principal regulator of fetal growth and fetal health. Typical placentas will grow uniformly out from the umbilical cord insertion, resulting in a round to oval disk with a centrally inserted cord. A variable maternal uteroplacental environment (the maternal “soil”) affects macroscopic placental structure as a change in shape. Where the maternal “soil” is not receptive, placentas will not grow, or not robustly. Irregularities in disk outline, umbilical cord insertion and in disk thickness are markers of fetal-placental environmental pathology, denoting variable placental arborization, and as such, deformation of normal placental growth resulting in an abnormal placental structure. The microscopic growth of the human placenta involves repeated branching, analogous to the roots of a tree; its mature arborization pattern is complex (e.g., [1-8]), so complex that it cannot be measured reliably even by expert, dedicated pediatric pathologists [9,10]. Just as the pattern of roots reflects the underlying soil’s fertility and predicts the health of plants that depend on those roots for sustenance, placental arborization reflects the health of the maternal environment and impacts on fetal health [11].

The typical shape of a human placenta is well-understood [12], however, there are many possible deviations from it. Shapes “other than round” can be difficult to classify; the Collaborative Perinatal Project used a variety of terms to attempt to describe such abnormal placental shapes but had to resort, after “bipartita” and “tripartite” to terms such as “multiplex” to convey the complexity of placental shapes. Such subjective and imprecise terminology has not advanced our understanding of the genesis of such shapes, and has limited our ability to analyze the relationship of abnormal placental growth shapes to the health of the fetus and child.

However, it is evident, that many atypically shaped placentas are quite regular, and can be classified into several well-defined geometrical patterns. This regularity suggests that there may be a common underlying pathological mechanism(s) responsible for much of the variability of observed shapes of placentas. In this work we propose such a mechanism: we derive the variability of placentas from a change in the branching structure of their vascular trees. To demonstrate how this may occur, we introduce a dynamic model for the growth of the vascular tree of a placenta. This model is based on a biologically realistic random growth process. We then show how a change of the parameters of the growth at a single instance leads to the appearance of the observed variability of placentas.

MATERIALS AND METHODS

Placental Cohort

The *Pregnancy, Infection, and Nutrition Study* is a cohort study of pregnant women recruited at mid pregnancy from an academic health center in central North Carolina. Our study population and recruitment techniques are described in detail elsewhere [13]. Beginning in March 2002, all women recruited into the *Pregnancy, Infection, and Nutrition Study* were requested to consent to a detailed placental examination. As of October 1, 2004, 1,159 women (94.6 percent) consented to such examination. Of those women who consented, 1,014 (87.4 percent) had placentas collected and photographed for image analysis. Of the 1,014 consecutive placentas collected, two cases were excluded because the trimmed placental weight was not recorded, and six cases were delivered in fragments, such that measurement of chorionic plate landmarks was not possible. This left 1,008 cases for analysis, 99 percent of the available placental sample. Placental gross examinations, histology review, and image analyses were performed at *EarlyPath Clinical and Research Diagnostics*, a New York State-licensed histopathology facility under the direct supervision of Dr. Salafia. The institutional review board from the University of North Carolina at Chapel Hill approved this protocol.

The fetal surface of the placenta was wiped dry and placed on a clean surface after which the extraplacental membranes and umbilical cord were trimmed from the placenta. The fetal surface was photographed with the Lab ID number and 3 cm. of a plastic ruler in the field of view using a standard high-resolution digital camera (minimum image size 2.3 megapixels). A trained observer (D.H.) captured series of x, y coordinates that marked the site of the umbilical cord insertion, the perimeter of the fetal surface, and the “vascular end points”, the sites at which the chorionic vessels disappeared from the fetal surface. The perimeter coordinates were captured at intervals of no more than 1 cm, and more coordinates were captured if it appeared essential to accurately capturing the shape of the fetal surface. The chorionic vessels extend out from the umbilical cord insertion and, at varying intervals from the edge of the fetal surface, dive beneath the surface so that they are no longer visible. Those “vascular end points” mark the terminal differentiation of the chorionic vessels into fetal stems and the finer structures of the placental functional units (P. Kaufman, MD, personal communication).

Computer software

Numerical simulations of vascular trees were carried out using *dla-3d-placenta*, a Unix-based, ANSI C, 3-dimensional, diffusion-limited aggregation simulation package. In its development, we have used Mark Stock’s *dla-nd* arbitrary-dimensional diffusion-limited aggregation simulator, a free software developed under the terms of the GNU General Public License as published by Free Software Foundation. For DLA cluster visualization we have used *PovRay*: a freeware ray tracing program available for a variety of computer platforms.

Random number generators

Random number generators used in this study include:

- drand48, an ANSI C system-supplied double-precision linear congruential uniform number generator, (generates sequence of integers I_1, I_2, I_3, \dots , each between 0 and M by the recurrence relation $I_{n+1} = aI_n + c \pmod{M}$).
- ran1(long *idum), uniform random number generator of Park and Miller with Bays-Durham shuffle and added safeguards [14].
- ran2(long *idum), long period random number generator of L’Ecuyer with Bays-Durham shuffle and added safeguards [14].

Seeing Stars (I)—The typical shape of a placenta is round, with the umbilical cord insertion roughly at the center [12], as illustrated in Fig. 1 (left column). We also calculated the *mean* shape of a placental surface in our dataset. The insertion point of the umbilical cord was placed at the origin, and the point on the perimeter closest to the rupture of the amniotic sac was positioned on the negative vertical axis, for consistency. The perimeters were rescaled to a common size. The points in the perimeter were then averaged inside a sector of 18° , thus obtaining 20 radial markers for each placenta. Each of the markers was then averaged over the whole dataset, thereby giving 20 mean placental radii from the umbilical insertion point spaced at 18° angular intervals. They were further averaged to obtain the mean average placental radius. The 20 mean radii were within 5% of the average placental radius, with the standard deviation from the average equal to 1.8%. Thus, the mean shape is round, with a centrally inserted umbilical cord. We aim to explain some of the variability from the round-oval shape, concentrating on two regular shapes which appear prevalent:

- Star-shaped placentas (about 5% of all cases). A typical star has between 5 and 7 prominent spikes. Variability of the radius of a star, as measured from the umbilical cord, is typically within 20 – 30% (Fig.1, middle column).

- Several pronounced lobes. These placentas also account for about 5% of the total cases. The number of lobes is typically 2 or 3 (Fig. 1, right column).

We propose to explain this observed variability by a deviation in the growth of the vascular tree of the placenta. In the next section we introduce a dynamic growth model for a vascular network. We then demonstrate how the model explains the observed shapes, and present evidence to support our explanation.

A note on the existing models of vascular trees—Numerous *static* models of vascular trees exist in the literature (see e.g. [15] and references therein). They are usually based on various optimization algorithms for filling the spatial structure of an organ. Such an approach is, however, completely unsuitable for our purposes. We aim to demonstrate how a deviation in the process of the *dynamical* growth of the vascular network affects the macroscopic shape of a placenta. We thus present a *dynamic* model of growth of a vascular tree. Local models of angiogenesis exist in previous literature (see [16], for example), however, they do not take into account the global vascular tree structure and only describe a growth of a single “strand” of the tree — which is again unsuitable for us.

Modeling growth at the tips, or a cloud of blind flies—Growth of blood vessels is recognized to depend on the concentration gradients of appropriate growth factors. Cells situated at the tip of vascular sprouts sense and navigate the environment, while cells in the sprout stalks proliferate and form a vascular lumen [17], [18], [19]. How do we model the new growth of a vascular tree at the tips of the branches? For simplicity, let us discretize both time and the units of growth. For a three-dimensional tree we should then ask where its tips are, to determine where the growth is likely to occur in the next unit of time. While this does not appear to be a simple task even for a tree with a few branches, there is a general (and easily automated) method for doing this.

For illustration, consider a tree. At some distance from the tree, release a cloud of blind flies. Flying randomly, without any sense of direction, our flies will only stop when they come in contact with the tree. At this point, a fly would close its wings, and sit at the spot where the contact occurred. It is a remarkable mathematical fact that:

It is one of the tips of the tree, where a fly is most likely to land (see Fig. 2).

We can thus identify the tips as the places with the most flies, and the relative number of flies which have landed at a given extremity will correspond to the likelihood that the next unit of growth will happen there.

To formulate this in more precise terms, let us select as a unit of growth (which we will call a *particle*), a three-dimensional ball of a small diameter d . At each moment of time our tree grows by one particle. At the initial time $t=1$, we start with a tree C_1 consisting of a single particle. Thus, at time n , our tree is a *cluster* C_n consisting of n particles. To grow it by one unit, consider a large sphere S around C_n (much larger than the size of the cluster itself). Randomly select a point w in S , as the initial position of a blind fly. The fly will perform a *random walk* (or a random flight in this case) originating from w . That is, it will randomly perform a sequence of moves up/down, left/right, forward/backward. Recording its spatial positions, we will see a sequence of points

$$W_0 = w, W_1, \dots, W_{t-1}, W_t, \dots$$

where w_t is produced from w_{t-1} by adding an increment s_t . The increment always has the same size, comparable to d (to fix the ideas, we can take it equal to d). The direction of the increment has to be aligned with one of the three coordinate axes (up/down, left/right, forward/backward) and randomly chosen from the six possibilities.

If at some point of time t the point w_t is at a distance of less than $2d$ from the cluster C_n , then we attach a new particle to this position, and thus obtain a bigger cluster C_{n+1} . If before this happens, the particle w_t drifts outside of the large sphere $2S$, then we discard it, and select a new initial point w .

Such random growth, first introduced by Witten and Sander in 1981 ([20], [21]), is known to physicists under the somewhat unwieldy name *Diffusion Limited Aggregation*, or *DLA* for short.

Visualizing a DLA tree as a vascular network—A tree C_n constructed in this way consists of n three-dimensional balls, all with the same small diameter d . To visualize it consistently with the structure of a vascular network, we need to make some of the branches thicker, and the other thinner. We first identify its branch structure in the following way. We say that a particle x is an immediate descendant of a particle y , if x is attached to y , and y is older than x . Further, x_n is a descendant of $x=x_0$ if there is a chain of DLA particles

$$x_0, x_1, \dots, x_{n-1}, x_n$$

such that x_i is an immediate descendant of x_{i-1} for $0 < i \leq n-1$. Now we can assign a visualization size v to each DLA particle, consistently with the principle, that bigger vessels grow first. Specifically, let the weight m of a particle x be the total number of its descendants. Thus, older particles, which are located closer to the root (the very first particle C_1) of the DLA tree, will have a larger weight. We then assign

$$v = e^{am}$$

with a suitably chosen parameter a to visualize the model vascular tree. Changing the diameter of each DLA particle to its visualization size v we obtain a model vascular tree with the thickness of branches varying consistently with the structure.

Growing denser trees—Our model has a single parameter $0 < \kappa \leq 1$ which will be completely crucial to our study. It is the probability that a DLA particle will stick to the cluster when it collides with it. Think again of a blind fly which has encountered one of the tips of the tree. If $\kappa \neq 1$, then with non-zero probability $1-\kappa$ the fly will continue its travels. Most likely, it will end up sitting at some nearby point of the tree, but not necessarily at the tip. The effect of this is to add some diffusion to DLA growth. The smaller the value of κ is, the more “hairy” the resulting tree will become.

From modeling considerations, it is also useful to note that the physical size d (as opposed to the visualization size) of a DLA particle can be changed during the growth of the cluster. This is a quick and dirty way of changing the branching structure. A smaller particle will also tend to diffuse along the tips of the DLA cluster formed by larger particles, hence a reduction of d will create more branching.

Growing a human placenta with DLA—To model the growth of a placental vascular tree, we surround our growth with a spherical constraint, modeling the walls of the uterus. The constraint absorbs any DLA particle which hits it from the interior, thus ensuring that no growth penetrates the constraint. The initial cluster marks the insertion of the umbilical cord. It is placed near the “south pole” of the constraint.

To ensure that the initial growth is directed towards the constraint (the umbilical cord does not grow away from the wall of the uterus), it is helpful to select the initial cluster C_1 consisting not of one, but of several DLA particles. The number of particles in C_1 is still insignificant, compared with the overall size of the DLA growth (in our experiments, it is between 0.01-1% of the total). We have experimented both with a deterministically defined C_1 , and with a short

initial cluster given by an opportune DLA growth, with identical results. The total number of DLA particles in a grown model vascular tree is between 150-200 thousand.

Once the parameters, such as the position and the shape of the initial cluster have been chosen, the model was tested by varying the random number generator (RNG) used to grow DLA. We have tested the model in two ways: by changing the “seed” of a given RNG (this changes the random number sequence but not the algorithm which produces it); and by changing the RNG itself. The results were very robust (Fig. 3).

Seeing Stars (II)—To produce models of placentas of irregular shapes we have varied the branching parameter κ of the growth at various stages of the development of the model placenta. A single instance of the change in the value of κ over the course of growth of the model is required to produce the observed variability (see Fig. 4):

- Decreasing the branching parameter κ (by a multiple 0.01) at an early stage of the growth (after 5-7% of DLA particles have attached) leads to a picture with several (typically two or three) large lobes. Qualitatively, the large vessels grow apart early, and with an increased degree of branching, the tree does not produce enough “medium size” branches to uniformly fill a circular shape (Fig.4, middle column).
- Well-defined stars with 5-7 pronounced arms correspond to a change of branching at a late stage of growth (typically after 50% of DLA particles have attached). We have achieved this result by decreasing κ , and alternatively, by decreasing the physical size of the DLA particle (Fig. 4, right column). Changing the physical size of a DLA particle turns out to be a more convenient parameter here (the size was typically decreased by 20%).

As further comparison of model shapes, we calculate the mean distance of a small vessel to the point of insertion of the umbilical cord in a sector of 5° , which is then rotated in increments of 2.5° . In each of the 5° sectors, we then mark the point on the bisector, whose distance to the vertex is equal to the mean distance for this particular sector. Connecting these points by line segments, we obtain a diagram, tracing the shape of the model placenta. The diagrams in the bottom row of Figure 4 correspond to the model placentas above them, in the third row of the same figure.

A further evidence for the mechanism of star formation we are describing is found in the variability of thickness of star-shaped placentas. A change in the density of the vascular tree is going to correspond to changing thickness of the placenta. Thus in a “star”, the arms will be thicker than the areas between them. In a vertical slice, this would produce a wavy pattern, schematically shown in Fig. 5 (top).

In Fig. 5 we demonstrate vertical slices of placentas taken at 1cm intervals. First is a typical placenta, with slices exhibiting uniform thickness. Next are pictures of slices of stars, with a wavy pattern clearly visible.

Further evidence that variable shapes reflect the architecture of the vascular fractal: deviations from the $\frac{3}{4}$ rule—The $\frac{3}{4}$ rule (or *Kleiber's Law*) is a famous allometric scaling law, which postulates that the basic metabolic rate B and the body mass M are related as

$$BM^{3/4}.$$

If the vascular system consisted of thin tubes of small size, uniformly filling the volume of the body, one would expect the two variables to be proportional. The appearance of a power $\frac{3}{4}$ is explained by the fractal structure of the vascular tree (see e.g. [22]). The fact that the same

power law is observed in many different organisms, suggests a universality of vascular architecture. Some explanations of this universality (such as the model in [22]) have appeared in the literature.

We have verified this scaling law for human fetuses, using the placental weight as a proxy for the basic metabolic rate ([23]). This results in an allosteric scaling equation

$$\log [\text{placental weight}] = \log \alpha + \beta \cdot \log [\text{birth weight}], \quad (*)$$

in which β represents the unknown power. The calculated value of β was 0.78 ± 0.02 in an excellent agreement with the rule.

Our DLA model is premised on the shape of the placenta reflecting an underlying vascular fractal. It is thus reasonable to expect, that a deviation from the typical round shape of a placenta with a central insertion of the umbilical cord will be correlated with abnormal placental vascular architecture. The latter should result in a deviation from the normal value of $\beta \approx 3/4$.

To test this prediction, we have employed several measures of deviation from a round placental shape. Firstly, we have calculated the standard deviation of the radius, measured from the point of insertion of the umbilical cord. For a round placenta with a central insertion, this value is 0. However, this measure will not differentiate between a regular ellipse and a star. We have used another simple measure, the *roughness*, calculated as the perimeter of the shape divided by the perimeter of the smallest convex hull that contained the shape. It is equal to 1 for any convex shape, such as a circle. Descriptive statistics determined the percentage with values for both parameters within 10% of the values for a round circle (0, 1 respectively), and for the subsequent deciles of deviation.

In Table 1 the results of Spearman's rank correlations are presented for our dataset. The variable *OutSdRCrd* is the deviation of the radius from the point of insertion, *OutRough* is the roughness. Both of them are significantly correlated with the variable β which is the difference between the computed value of β from the scaling equation (*), and the "ideal" value 0.75. The inverse (-) association of the radial deviation and β means that as the deviation increases the difference between β observed and 0.75 is greater.

Our interpretation is confirmed by the lack of correlation of the variable *OutSdR* (the standard deviation of the radius calculated from the centroid of the placental shape) with the deviation from 0.75. This is as we predict, since the centroid of the placental shape is an arbitrary geometrical center that does not directly relate to the underlying vascular architecture that ramifies out from the umbilical cord insertion site.

CONCLUSION

We have presented a mechanism which accounts for two of the most common patterns of abnormal placental shapes (multilobate placentas and star-shaped placentas), specifically, changes in the arborization of the vascular tree. To confirm it, we have developed a dynamic model of growth for the vascular tree based on a DLA random growth process. We have demonstrated that the observed variability of shapes is explained by a change of the arborization parameter of the model at a single time instance. Thus, the time in gestation of determination of these two patterns may be distinct.

In addition, we have empirical evidence that the shape of the placenta does reflect the underlying vascular fractal; deviations from symmetric fractal expansion out from the umbilical cord insertion are associated with reduced placental functional efficiency, i.e., a smaller birth weight for the given placental weight. We speculate that these deviations reflect placental compensations responding to stressors or variability in the maternal environment.

The use of a fractal model of this type is reasonable to model the placenta. Its structure is little more than a thin tissue sheath covering a complex arborizing vascular network. Our empiric data are consistent with its function being intimately dependent on its structure, suggesting that our model will be germane to any studies of birth weight as a measure of the adequacy of the intrauterine environment. Restriction of placental vascular outgrowth is a potent model of fetal growth restrictions [24]. Placental growth within the uterine lining has been likened to tumor growth for decades [25]. Fractals have likewise proved fruitful to analysis of retinal vasculature architecture [26] as well as the vascular structure of the heart and brain [27]. As every mathematical model of a biological process, ours is based on several assumptions which may oversimplify the reality, and should be applied with some caution. It does provide an insight, however, into the connection between the placental spatial shape and the underlying vasculature, which invites further investigation.

Birth weight has been used as a proxy for the adequacy of the intrauterine environment in most studies of the fetal origins of adult health risks ([28-45]). Our findings correlate it with the placental shape and structure, and thus may be helpful in studies of the relationship of intrauterine stressors to the fetal modifications that are believed to underlie these lifelong health risks.

ACKNOWLEDGMENT

This project was started during 2007 Program “Random Shapes” at the Institute for Pure and Applied Mathematics at UCLA, where C.S. and M.Y. were Core participants. We gratefully acknowledge the support of IPAM, and thank the organizers of the program for bringing us together. M.Y. would like to thank two other participants, Ilia Gruzberg and Ilia Binder for useful discussions of DLA.

This work was partially supported by NSERC Discovery Grant (M. Yampolsky), by NARSAD Young Investigator Award (C. Salafia), by K23 MidCareer Development Award NIMH K23MH06785 (C. Salafia).

REFERENCES

- [1]. Kaufmann P, Mayhew TM, Charnock-Jones DS. Aspects of human fetoplacental vasculogenesis and angiogenesis. II. Changes during normal pregnancy. *Placenta* 2004;25(23):114–26. [PubMed: 14972444]
- [2]. Kusanke G, et al. Branching patterns of human placental villous trees: perspectives of topological analysis. *Placenta* 1993;14(5):591–604. [PubMed: 8290498]
- [3]. Kaufmann P, Sen DK, Schweikhart G. Classification of human placental villi. I. Histology. *Cell Tissue Res* 1979;200(3):409–23. [PubMed: 487407]
- [4]. Kingdom J, et al. Development of the placental villous tree and its consequences for fetal growth. *Eur J Obstet Gynecol Reprod Biol* 2000;92(1):35–43. [PubMed: 10986432]
- [5]. Charnock-Jones DS, Kaufmann P, Mayhew TM. Aspects of human fetoplacental vasculogenesis and angiogenesis. I. Molecular regulation. *Placenta* 2004;25(23):103–13. [PubMed: 14972443]
- [6]. Mayhew TM, Charnock-Jones DS, Kaufmann P. Aspects of human fetoplacental vasculogenesis and angiogenesis. III. Changes in complicated pregnancies. *Placenta* 2004;25(23):127–39. [PubMed: 14972445]
- [7]. Demir R, et al. Fetal vasculogenesis and angiogenesis in human placental villi. *Acta Anat (Basel)* 1989;136(3):190–203. [PubMed: 2481376]
- [8]. Benirschke, K, KP. *The Pathology of the Placenta*. Springer-Verlag; New York: 2002. *Angioarchitecture of Villi*; p. 134-140.
- [9]. Grether JK, et al. Reliability of placental histology using archived specimens. *Paediatr Perinat Epidemiol* 1999;13(4):489–95. [PubMed: 10563368]
- [10]. Khong TY, et al. Observer reliability in assessing placental maturity by histology. *J Clin Pathol* 1995;48(5):420–3. [PubMed: 7629287]
- [11]. Khong TY. Placental vascular development and neonatal outcome. *Semin Neonatol* 2004;9(4):255–63. [PubMed: 15251142]

- [12]. Benirschke K, KP Architecture of Normal Villous Trees, Chapter 7. Pathology of the Human Placenta 2002;116:154 Springer Verlag New York, New York.
- [13]. Savitz DA, Dole N, Williams J, et al. Determinants of participation in an epidemiological study of preterm delivery. *Paediatr Perinat Epidemiol* 1999;13:114–25. [PubMed: 9987790]
- [14]. Press, WH., et al. Numerical recipes in C: the art of scientific computing. Cambridge University Press; 1992. p. 994
- [15]. Horst, K. Hahn; Manfred, Georg; Heinz-Otto, Peitgen. Fractal Aspects of Three-Dimensional Vascular Constructive Optimization. In: Losa, G., et al., editors. *Fractals in Biology and Medicine*. Birkhäuser; Basel: 2005.
- [16]. Anderson ARA, Chaplain MAJ. Continuous and discrete mathematical models of tumour-induced angiogenesis. *Bull Math. Biol* 1998;60:857–899. [PubMed: 9739618]
- [17]. Gerhardt H, Betsholtz C. How do endothelial cells orientate? *EXS* 2005;(94):3–15. [PubMed: 15617467]
- [18]. Demir R, Seval Y, Huppertz B. Vasculogenesis and angiogenesis in the early human placenta. *Acta Histochem* 2007;109(4):257–65. [PubMed: 17574656]
- [19]. Reynolds LP, Borowicz PP, Vonnahme KA, Johnson ML, Grazul-Bilska AT, Wallace JM, Caton JS, Redmer DA. Animal models of placental angiogenesis. *Placenta* 2005 Nov;26:10689708 [PubMed: 16226119]
- [20]. Witten TA Jr, Sander LM. Diffusion-limited aggregation, a kinetic critical phenomenon. *Phys. Rev. Lett* 1981;47:1400–1403.
- [21]. Meakin P. *Fractals, Scaling and Growth Far from Equilibrium*, Cambridge Nonlinear Science Series 5, 1999 Cambridge University Press Cambridge, U.K.
- [22]. West GB, Brown JH, Enquist BJ. A general model for the origin of allometric scaling laws in biology. *Science* 1997;276:122–126. [PubMed: 9082983]
- [23]. Salafia CM, Misra DY, Yampolsky M, Charles AK, Miller RK. Allosteric metabolic scaling and fetal-placental growth Technical report 0805.3675 at <http://www.arXiv.org>
- [24]. Rutland CS, Mukhopadhyay M, Underwood SC, Clyde N, Mayhew TM, Mitchell CA. Induction of intrauterine growth restriction by reducing placental vascular growth with the angioinhibin TNP-470. *Biol Reprod* 2005 Dec;73:6116473 Epub 2005 Aug 3. [PubMed: 16079307]
- [25]. Ferretti CB, Brunil D, Angles-Marie V, Pecking AP, Bellet DM. Molecular circuits shared by placental and cancer cells, and their implications in the proliferative, invasive and migratory capacities of trophoblasts. *Hum Reprod Update* Mar-Apr;2007;13:212141 [PubMed: 17068222]
- [26]. Masters BR. Fractal analysis of the vascular tree in the human retina. *Annu Rev Biomed Eng* 2004;6:427–52. [PubMed: 15255776]
- [27]. Rossitti S. Energetic and spatial constraints of arterial networks. *Arq Neuropsiquiatr* Jun; 1995;53:233341 [PubMed: 7487549]
- [28]. Jaddoe VW, Witteman JC. Hypotheses on the fetal origins of adult diseases: contributions of epidemiological studies. *Eur J Epidemiol* 2006;21(2):91–102. [PubMed: 16518677]
- [29]. DE Boo H, Harding JE. The developmental origins of adult disease (Barker) hypothesis. *Aust N Z J Obstet Gynaecol* 2006;46(1):4–14. [PubMed: 16441686]
- [30]. Barker DJ. The developmental origins of insulin resistance. *Horm Res* 2005;64(Suppl 3):2–7. [PubMed: 16439838]
- [31]. Barker DJ. The fetal origins of type 2 diabetes mellitus. *Ann Intern Med* 1999;130(4 Pt 1):3224 [PubMed: 10068392]
- [32]. Adair L, Dahly D. Developmental determinants of blood pressure in adults. *Annu Rev Nutr* 2005;25:407–34. [PubMed: 16011473]
- [33]. Levitt NS, et al. Adult BMI and fat distribution but not height amplify the effect of low birthweight on insulin resistance and increased blood pressure in 20-year-old South Africans. *Diabetologia* 2005;48(6):1118–25. [PubMed: 15864536]
- [34]. Levitt NS, et al. An inverse relation between blood pressure and birth weight among 5 year old children from Soweto, South Africa. *J Epidemiol Community Health* 1999;53(5):264–8. [PubMed: 10396531]

- [35]. Barker DJ, Osmond C, Law CM. The intrauterine and early postnatal origins of cardiovascular disease and chronic bronchitis. *J Epidemiol Community Health* 1989;43(3):237–40. [PubMed: 2607302]
- [36]. Barker DJ, Martyn CN. The maternal and fetal origins of cardiovascular disease. *J Epidemiol Community Health* 1992;46(1):8–11. [PubMed: 1573367]
- [37]. Rich-Edwards JW, et al. Longitudinal study of birth weight and adult body mass index in predicting risk of coronary heart disease and stroke in women. *Bmj* 2005;330(7500):1115. [PubMed: 15857857]
- [38]. Lawlor DA, et al. Birth weight is inversely associated with incident coronary heart disease and stroke among individuals born in the 1950s: findings from the Aberdeen Children of the 1950s prospective cohort study. *Circulation* 2005;112(10):1414–8. [PubMed: 16129799]
- [39]. Cooper C, et al. Review: developmental origins of osteoporotic fracture. *Osteoporos Int*. 2005
- [40]. Gluckman PD, et al. Life-long echoes--a critical analysis of the developmental origins of adult disease model. *Biol Neonate* 2005;87(2):127–39. [PubMed: 15564779]
- [41]. Baik I, et al. Association of fetal hormone levels with stem cell potential: evidence for early life roots of human cancer. *Cancer Res* 2005;65(1):358–63. [PubMed: 15665314]
- [42]. Bellingham-Young DA, Adamson-Macedo EN. Prematurity and adult minor illness. *Neuro Endocrinol Lett* 2004;25(Suppl 1):117–25. [PubMed: 15735594]
- [43]. Nilsson E, et al. Fetal growth restriction and schizophrenia: a Swedish twin study. *Twin Res Hum Genet* 2005;8(4):402–8. [PubMed: 16176726]
- [44]. Willinger U, et al. Neurodevelopmental schizophrenia: obstetric complications, birth weight, premorbid social withdrawal and learning disabilities. *Neuropsychobiology* 2001;43(3):163–9. [PubMed: 11287795]
- [45]. JabbarzadehE, AbramsCF. Strategies to enhance capillary formation inside biomaterials: a computational study. *Tissue Eng* 2007 Aug;13:207386 [PubMed: 17590150]

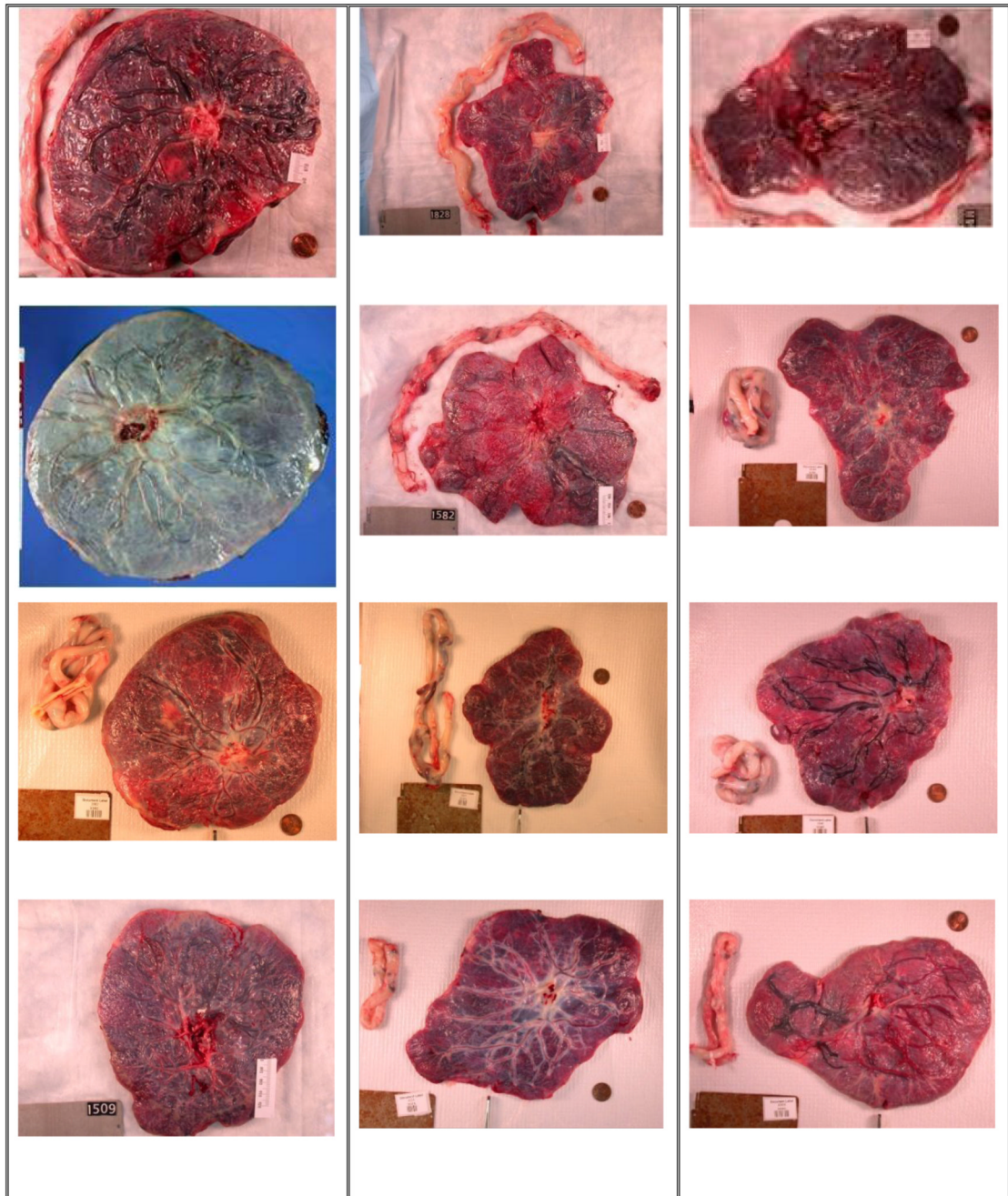


Figure 1. Placental shapes. Left column: normal round to oval shapes, middle column: “stars”, right column: multilobate shapes.

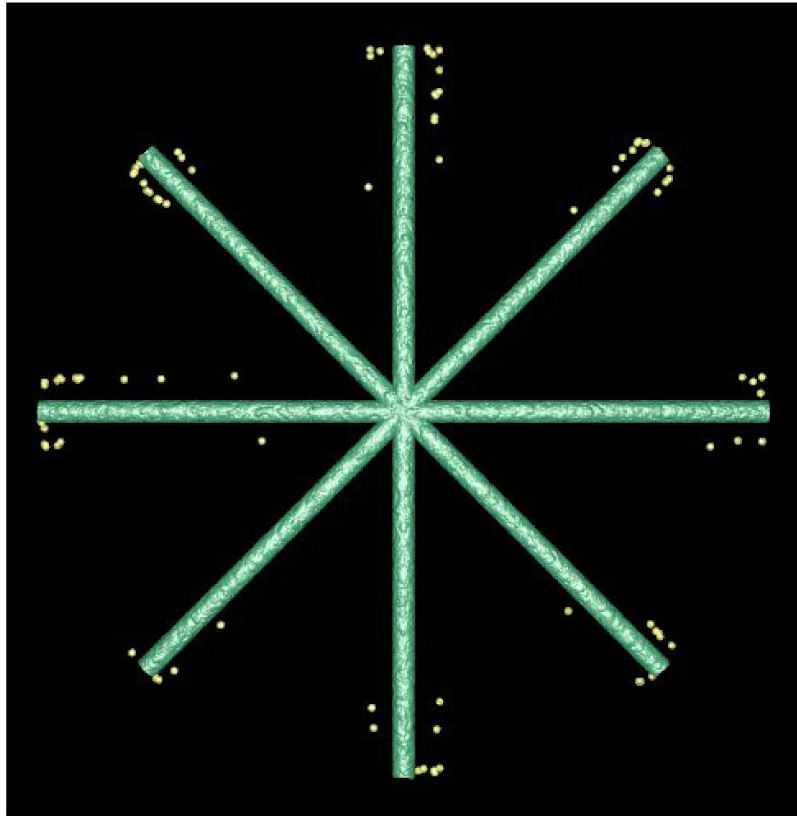


Figure 2. A tree with eight symmetric branches, and the positions where the first 100 "blind flies" land on it, generated by a numerical simulation (marked with dots).

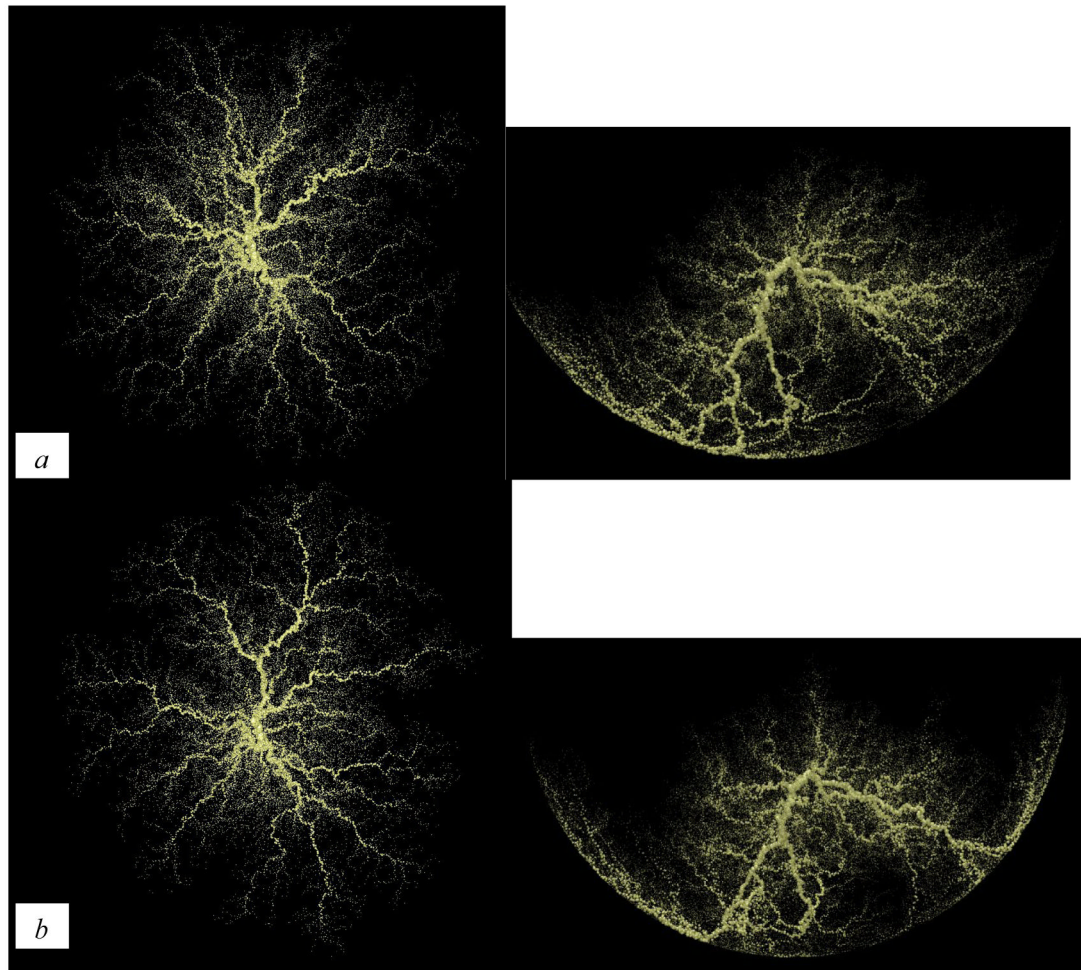


Figure 3. some examples of model vascular trees. On the left is an XY-plane projection, on the right is a YZ-projection. In the YZ-plane the spherical constraint is apparent.

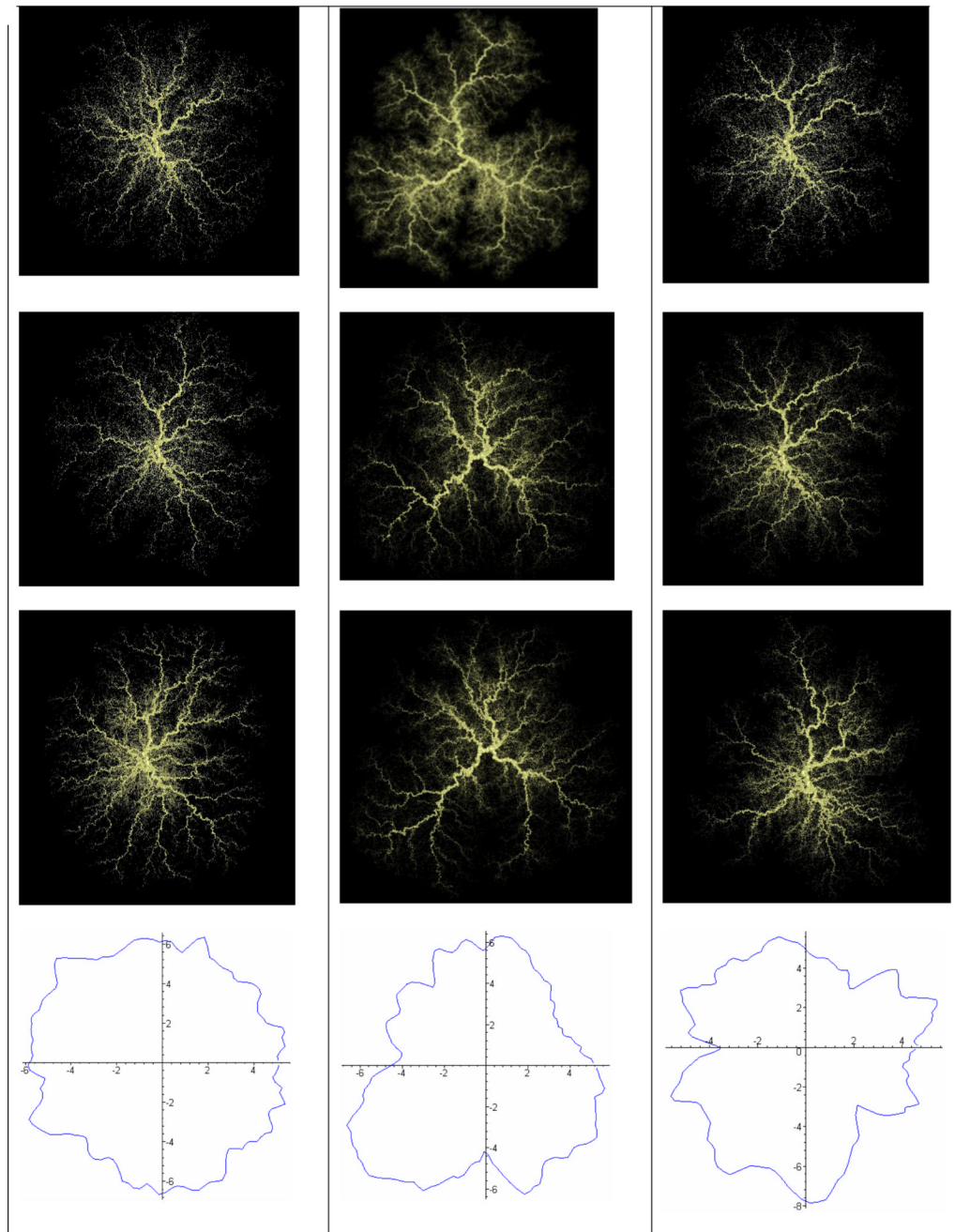


Figure 4. Model placentas of variable shapes. Left column: model normal placentas. Middle column: model three-lobate placentas. Right column: model star-shaped placentas. Bottom row: comparison of shapes. The average distance of a blood vessel to the point of insertion of the umbilical cord in a model placenta (marked in sectors of 5° , rotated in increments of 2.5°).

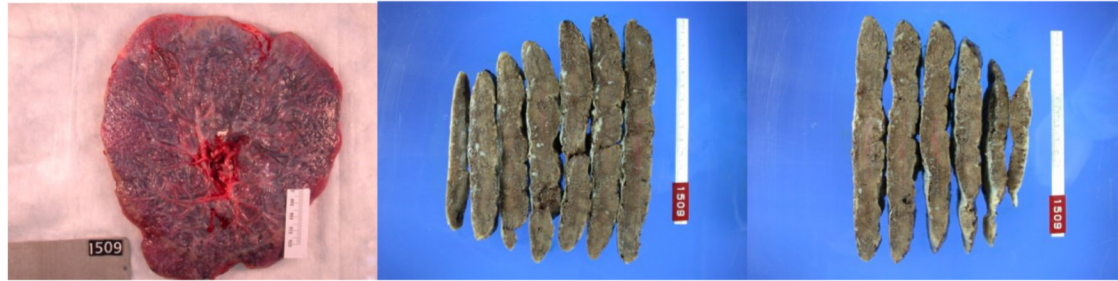
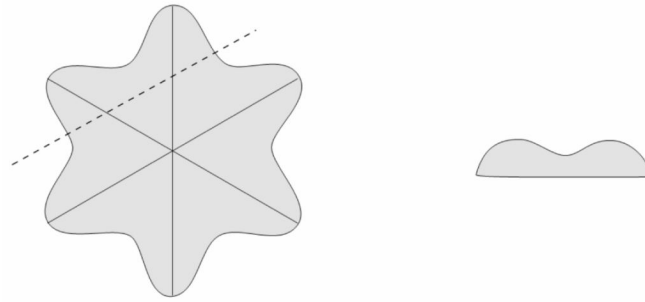


Figure 5. variable thickness of slices. Top row: the position of a vertical slice of a star is indicated schematically on the left, on the right is a drawing of the slice. Second row: the slices of a round placenta have uniform thickness. Third and fourth rows: slices of star-shaped placentas. The wavy shape of a slice is apparent.

Table 1

correlation of the deviation from a round shape with a deviation from the $\frac{3}{4}$ rule. Lower value of significance level means stronger evidence (e.g. 0.009 means 9 in a 1000 chance that the correlation happens by a coincidence).

| | | <i>$\Delta\beta$</i> |
|------------------|------------------------|--|
| <i>OutSdR</i> | Pearson Correlation | .020 |
| | Significance | .485 |
| | Number of measurements | 1199 |
| <i>OutSdRCrd</i> | Pearson Correlation | -.076 |
| | Significance | .009 |
| | Number of measurements | 1187 |
| <i>OutRough</i> | Pearson Correlation | .091 |
| | Significance | .002 |
| | Number of measurements | 1199 |